Biophysical Chemistry, 45 (1993) 227–234
Elsevier Science Publishers B.V., Amsterdam

BIOCHE 01714

Time-correlated models applicable to reactions in restricted geometries: phospholipid vesicles in their gel and liquid crystalline phases

Guy Duportail [a], Jean-Claude Brochon [b] and Panagiotis Lianos [c]

[a] *Centre de Recherches Pharmaceutiques, Laboratoire de Physique, UA CNRS 491: Université Louis Pasteur, B.P. 24, 67401 Illkirch Cedex (France)*
[b] *LURE, CNRS-MEN-CEA, Bat. 209d, Centre Universitaire Paris-Sud, 91405 Orsay (France)*
[c] *University of Patras, School of Engineering, Physics Section, 26110 Patras (Greece)*

(Received 22 April 1992; accepted in revised for 10 August 1992)

Abstract

The fluorescence decay profiles recorded with pyrene and with the fluorescence quenching process between diphenylhexatriene and 12-doxylstearic acid methyl ester in small unilamellar vesicles of dipalmitoylphosphatidylglycerol and L-α-phosphatidylglycerol have been analyzed with a model appropriate for reactions in restricted geometries. Measurements were made both in the gel and in the liquid crystalline phase, either by changing temperature or by changing the composition of a phospholipid mixture. We have found that in the gel phase, the reactions are more restricted, that is, they proceed more locally than in the liquid crystalline phase. The number of solubilization sites available to the reactants is much larger in the liquid crystalline phase than in the gel phase for pyrene, and it is much larger, tending to infinity, for the diphenylhexatriene–quencher couple. The probability of an immediate encounter between two reactants decreases from the gel to the liquid crystalline phase and as the temperature increases. In a short time scale of observation, the rate of the diffusion-controlled reaction increases with temperature and in going from the gel to the liquid crystalline phase. However, when the time scale is large, long-distance diffusion, even in the liquid crystal-line phase and at high temperature, is impossible.

Keywords: Fluorescence probing; Restricted geometries; Phospholipid vesicles

1. Introduction

Fluorescence probing, both steady-state and time-correlated, has yielded a lot of information on the structure and dynamics of lipid vesicles. In these studies, pyrene excimer formation has often been used [1,2]. The fluorescence decay profiles are then analyzed either as a sum of exponentials [3] or by utilizing a model based on the Einstein–Smoluchowski diffusion theory [4], involving a time-dependent diffusion coefficient. Here we add to the information obtained so far, by utilizing a universal model applicable to all

Correspondence to: Panagiotis Lianos, University of Patras, School of Engineering, Physics Section, 26110 Patras, Greece. Tel.: 30-61-997587, Fax: 30-61-991725.

lipid vesicles, by treating the lipidic core as an environment of restricted geometry. We use two fluorophore–quencher systems: pyrene, quenched by excimer formation, and the couple diphenylhexatriene–12-doxylstearic acid methyl ester [5]. The latter is very promising for probing lipid environments.

It has been previously shown [5–12] that the fluorescence decay profile in any restricted quenching reaction of the type A + B → products ([A] ≪ [B]) can be adequately described by the following equation:

$$I(t) = I_0 \exp(-k_0 t) \exp(-C_1 t^f + C_2 t^{2f}) \quad (1)$$

where k_0 is the decay rate constant in the absence of quenching, C_1 and C_2 are constants and f is a non-integer positive exponent, smaller than unity, proportional to the dimensionality of the reaction domain.

If the reaction between the excited fluorophore and the quencher is modeled as a random walk then f has an additional interesting feature. In random-walk terms, the reaction rate depends on the number of distinct sites $S(n)$ visited by the random walker performing n steps, which is given by $S(n) \sim n^f$, where $f = d_s/2 = d_f/d_w$. Then d_s is the spectral dimension, d_f the fractal dimension and d_w the fractal dimension of the random walk [13–16]. In this case the term $C_1 t^f$ is proportional to the average $S(t)$ while $C_2 t^{2f}$ is proportional to its variance [16].

The equivalent first-order reaction rate "constant" $K(t)$ is not constant but is obtained by the following equation:

$$K(t) = fC_1/t^{1-f} - 2fC_2/t^{1-2f} \quad (2)$$

The analysis of the fluorescence decay profiles allows the calculation of the parameters C_1, C_2 and f, and through eq. (2) the reaction rate $K(t)$.

In the present work we study the evolution of the quenching reaction in both the gel (GP) and the liquid crystalline phase (LCP) of small unilamellar vesicles (SUV) by utilizing two different lipids: dipalmitoylphosphatidylglycerol (DPPG) and L-α-phosphatidylglycerol (LαPG), and by varying the temperature. Small unilamellar vesicles at relatively low concentration (10^{-4} M) have been used in order to diminish scattered light from vesicles, though it cannot be completely eliminated.

2. Materials and methods

Dipalmitoylphosphatidylglycerol (DPPG), L-α-phosphatidylglycerol (LαPG) and 12-doxylstearic acid methyl ester (12-DSME) were purchased from Sigma and used without further purification. Anionic phospholipids were used because the resulting vesicles were much less turbid than vesicles obtained from phosphatidylcholine. Pyrene and diphenylhexatriene (DPH), scintillation grade, were purchased from Kodak.

Small unilamellar vesicles (SUV) were obtained from multilamellar vesicles. Aliquots of stock phospholipid solutions in chloroform were added to a 25 ml round-bottom flask and the volume was brought to about 5 ml with chloroform. The sample was then dried as a thin film by rotary evaporation, and the vacuum was maintained for 30 min to remove any residual solvent. The lipid film was then dispersed in a phosphate buffer (100 mM, pH 7) at 50°C (10°C higher than the phase transition temperature of DPPG), by vigorous vortex shaking for 2 min, giving a multilamellar vesicles dispersion. This dispersion was sonicated for 90 min under nitrogen, at the same temperature, in a bath-type sonicator (Bransonic 320, 120 W), to obtain small unilamellar vesicles. The average diameter of the vesicles was 70 nm, whatever the lipid concentration, as measured by photon correlation spectroscopy (Coulter particle analyzer N4 SD). These vesicles were used without further treatment. The phospholipid concentration was kept at 10^{-4} M.

The concentrations of the probes (pyrene, DPH, 12-DSME) in the samples were infered from the concentrations of organic stock solutions. Aliquots of these stock solutions were directly added to the chloroformic solutions before evaporation. The concentration of pyrene embedded into the vesicles was checked by absorption. We have previously shown [12] that pyrene absorbances for the labelled vesicles were proportional to the amount of added pyrene, up to 20

mol%, involving a total incorporation. In the present work pyrene concentration was kept at 2×10^{-5} M, giving a substantial quenching of monomer fluorescence [5,12]. DPH was kept at 10^{-6} M, and can be considered as totally embedded into vesicles [17]. This is probably not the case with 12-DSME, kept at 1.5×10^{-5} M, as the membrane partition coefficients for doxylstearates were shown to be about two orders of magnitude lower than the aromatic hydrocarbons, like DPH or pyrene [18]. To know the exact incorporation ratio of 12-DSME would necessitate a specific study beyond the scope of the present work, but what is important is to check that this quencher is enough embedded to also cause a substantial quenching of DPH fluorescence [5].

Steady-state fluorescence spectra were recorded with a SLM-48000 spectrofluorometer.

The fluorescence decay profiles of monomer pyrene were recorded with a time-correlated photon-counting apparatus equipped with a high-pressure hydrogen flash (8 bar). The excitation wavelength (321 nm) was selected by a Bausch & Lomb monochromator. The pyrene monomer fluorescence emission was selected by a 385 nm Schott interference filter. To avoid quenching by oxygen, all pyrene-containing samples were deoxygenated by bubbling nitrogen for 30 min. The decay time of pyrene monomer (without excimer) was measured on samples having a pyrene concentration low enough ($< 10^{-6}$ M) to diminish to the lowest possible minimum the probability of excimer formation. Further decrease of pyrene concentration would have created serious problems of accuracy of the recorded fluorescence data.

The fluorescence decay profiles of DPH were also recorded with the photon-counting technique. The experimental set up was installed on the SA1 beam line of the Synchrotron radiation of the Super-ACO of LURE, Orsay, France. The storage ring provided a light pulse with FWHM of 500 ps at a frequency of 8.33 MHz for a double bunch mode. The excitation and emission wavelengths were set at 360 and 435 nm, respectively, using Jobin-Yvon H25 monochromators. Figure 1 shows a fluorescence decay profile of DPH in

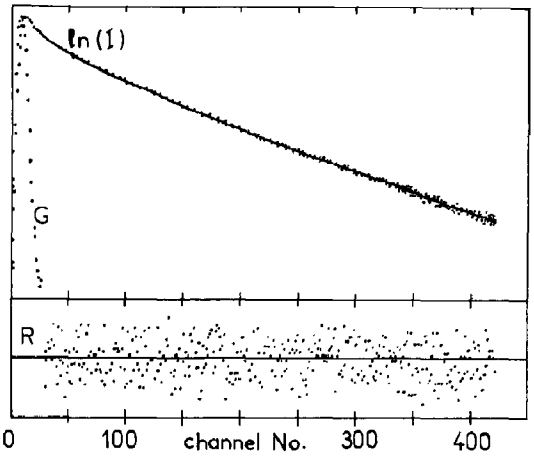

Fig. 1. Fluorescence decay profile of 10^{-6} M DPH in the presence of 1.5×10^{-5} M 12-DSME in DPPG vesicles at 20°C, together with fitted curve, exciting pulse (G) and residuals (R).

DPPG vesicles together with excitation pulse for comparison.

All fluorescence decay profiles were analysed with least-squares fits by using the standard fitting criteria, i.e. the distribution of the residuals, the autocorrelation value of the residuals and the chi-square values. Equation (1) was fitted to the experimental data after convolution with the excitation pulse according to the following equation:

$$F_i = A\left[\sum_{j=1}^{i} G_j \exp\{-k_0 w(i-j)\} \times \exp\{-C_1[w(i-j)]^f + C_2[w(i-j)]^{2f}\}\right] \quad (3)$$

where F_i corresponds to the experimental value of the fluorescence intensity at channel i, A is a fitted parameter, G_j is the value of the intensity of the exciting pulse at channel j and w is the interval between two channels (1.87 ns for pyrene and 0.116 ns for DPH). The fitting started 30 channels after the point where the exciting pulse starts rising, in order to avoid interference from scattered light. Of course, this choice was made at some expense of the information contained in

these first 30 channels. However, we believe that it does not dramatically affect our results. At any rate, the scattered-light interference would have produced much greater error.

3. Results and discussion

Table 1 shows the results of the analysis of the fluorescence decay profiles of 2×10^{-5} M pyrene solubilized in SUV of DPPG. The first column shows the temperature at which measurements were made. The GP to LCP transition for DPPG occurs at 41°C. Therefore, Table 1 shows the way an excited pyrene molecule interacts with an unexcited one, both in a "rigid" and in a "fluid" environment. The second column contains the values of the fluorescence decay time of free pyrene monomer. Notice that τ_0, decreases as the temperature increases. Such decrease can be explained by the fact that non-radiative decay processes are enhanced at higher temperature. However, the τ_0 values obtained with the present lipid concentration were substantially smaller than those previoulsy recorded with higher lipid concentration [12]. This indicates that some quenching effect, caused by excimer formation not detectable by steady-state fluorescence, might be responsible for such difference. We have made the present analysis always bearing this fact in mind, as well as the possibility that at high temperature non-specific processes, such as new type of collisional processes, might effect τ_0. We believe that, whatever the case, the present analysis is not affected. The τ_0 values have been used to calculate k_0, necessary for the analysis with eq. (3). Column No. 3 gives the values of the non-integer exponent of time f. The exponent f gives an estimate of the geometrical restrictions imposed by the environment on the excimer-forming reaction, which is considered to be diffusion-controlled. When the reaction occurs locally, i.e. when it is a quasi-stationary reaction, f takes very low values. Thus aggregated reactants should give very low f values [11,12]. f is large when the largest part of the reaction occurs by diffusion over relatively long distances. Large f values definitely preclude reactant aggregation. It is then interesting to note that relatively small f values are obtained below 41°C. f increases extensively in going above 41°C. Obviously, in the GP, the reaction domain is very restrictive. Then the reactants are compartmentalized in limited areas and the main part of the reaction occurs locally. On the contrary, in the LCP the reaction occurs by diffusion over some distance. More space is then allowed to the reactants and the geometry is less restrictive. It is interesting to compare this result with the information given by the spectra of Fig. 2. Notice that both the excitation spectrum and the emission spectrum are the same with those expected in non-restricted geometries, i.e. it is impossible to say by looking at these spectra whether the reaction accurs locally or by diffusion. It is then obvious that the time-correlated analysis presented here offers information that can not be obtained by other methods. Column No. 4 shows the parameter ratio C_1/C_2. These values, which compare C_2 with C_1, give information on two aspects: they increase as the geometry of the reaction becomes less restrictive and as the number of reactants over the number of the

Table 1
Data obtained by the analysis of the fluorescence decay profiles of 2×10^{-5} M pyrene in 10^{-4} M DPPG vesicles vs. temperature, using eqs. (1)–(3)

T (°C)	τ_0 (ns)	f	C_1/C_2	Rate constants (10^6 s^{-1})		
				K_1	K_{AV}	K_L
20	231	0.35	18	149	3.8	0
30	215	0.35	32	183	3.8	0
40	208	0.58	62	80	3.0	0
50	180	0.64	91	58	2.9	0
60	161	0.62	87	41	1.9	0

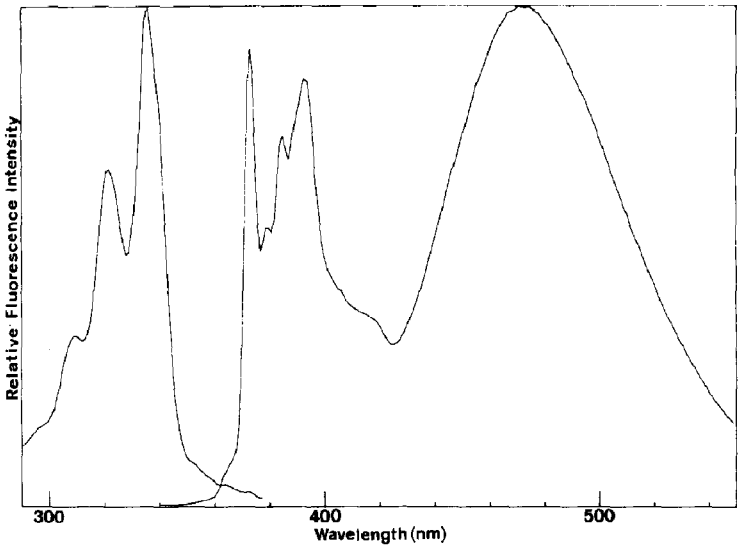

Fig. 2. Fluorescence excitation (left) and emission (right) spectrum of 2×10^{-5} *M* pyrene embedded in 10^{-4} *M* DPPG small unilamellar vesicles. The excitation wavelength for the emission spectrum was 321 nm with 2 nm emission slits. The emission wavelength for the excitation spectrum was 385 nm with 2 nm excitation slits.

available solubilization sites decreases. The increase of C_1/C_2 with temperature agrees with the increase of f. It is also consistent with the previous assertion that more space is allowed to the given number of reactants at higher temperatures. Finally, the three last columns of Table 1, show values for the constants, K_1 K_{AV} and K_L. These are three representative constants showing the way the first-order rate $K(t)$ evolves with time [5,12]. K_1 is the value of $K(t)$ at the beginning of the reaction and K_L at the end (i.e. at the last recorded channel), while K_{AV} is the average over 500 time-channels. K_1 is always larger than K_{AV} and K_L, particularly, when f is small [5,12]. Note that K_1 values are larger in the GP than in the LCP. K_1 shows the probability of the reaction immediately after the shining of the exciting pulse. Then its values are consistent with the above conclusions that, in the GP, quasistationary reactions take place, while such reactions are much less probable in the LCP and become even less probable with further temperature increase. K_L were all practically zero, i.e. substantially smaller than K_{AV} and very much smaller than K_1. This indicates that in the present DPPG vesicles and in the time scale monitored by pyrene fluorescence, reaction by diffusion at relatively large distances is precluded. With K_L being zero and K_1 decreasing with increasing temperature, K_{AV} is, naturally, also decreasing.

Table 2

Data obtained by the analysis of the fluorescence decay profiles of 10^{-6} *M* DPH in the presence of 1.5×10^{-5} *M* 12-DSME in 10^{-4} *M* DPPG vesicles vs. temperature, using eqs. (1)–(3)

T (°C)	τ_0 (ns)	f	C_1/C_2	Rate constants (10^7 s^{-1})		
				K_1	K_{AV}	K_L
20	11.1	0.38	25	115	5.2	1.7
30	11.1	0.45	19	105	5.3	1.4
35	11.0	0.49	32	108	7.6	2.8
40	9.1	0.62	342	68	10.9	6.7
45	8.7	0.61	1195	78	12.6	7.8
50	8.0	0.63	2952	78	14.8	9.5
60	7.5	0.66	∞	89	21.3	14.3

Table 2 shows the results of the analysis of the fluorescence decay profiles of 10^{-6} M DPH in the presence of 1.5×10^{-5} M 12-DSME both solubilized in SUV of DPPG. The temperature was again varied from 20 to 60°C. DPH decays much faster than pyrene. The decay profiles of free DPH in DPPG can be fitted by a sum of two exponentials, in good agreement with what is commonly observed in other membrane or vesicle systems. The values of τ_0 shown in Table 2 correspond to the longer-lifetime component. The significance of the shorter component may be a matter of controversy, but the results of Parassasi et al. [19], which seem to us convincing, attribute it to a photolytic process involving DPH and phospholipids. Thus the origin of this short component is independent of the physical state of the vesicle itself. Due to this reason and to the limited contribution of the short component we have adopted the long lifetime as the inverse of k_0 for DPH [5]. Note that, as it happens with pyrene, τ_0 decreases with increasing temperature. Both the absolute values and the type of variation of f observed with pyrene, agree with the corresponding f-values of Table 2. We thus verify that the reaction occurs locally in the GP, while in the LCP the geometrical restrictions are relaxed. Again, the excitation and emission spectra shown in Fig. 3 can not distinguish the type of interaction as given by time-correlated analysis. The values of C_1/C_2 of column No. 4, again, increase with temperature, as also observed with pyrene. However, the increase now is very large. At 60°C, C_2 is practically zero, compared to C_1. Since the geometry of the reaction, as indicated by the values of f, is sensed to be the same by both pyrene and DPH–12-DSME, we conclude that this extensive increase of C_1/C_2 reveals a very large increase of the number of available solubilization sites for the system DPH–12-DSME. In other words, 12-DSME which, being an amphiphilic molecule itself, must participate in the vesicle structure, has an infinite choice of positions with respect to DPH at high temperature, contrary to what happens to an excited pyrene molecule with respect to an unexcited one under the same conditions. Column No. 5 shows corresponding K_1 values. It must be stressed at this point that the uncertainty over the 12-DSME degree of incorporation into the vesicles (see Section 2) does not affect these K values since they are of the first-order, i.e. their calculation

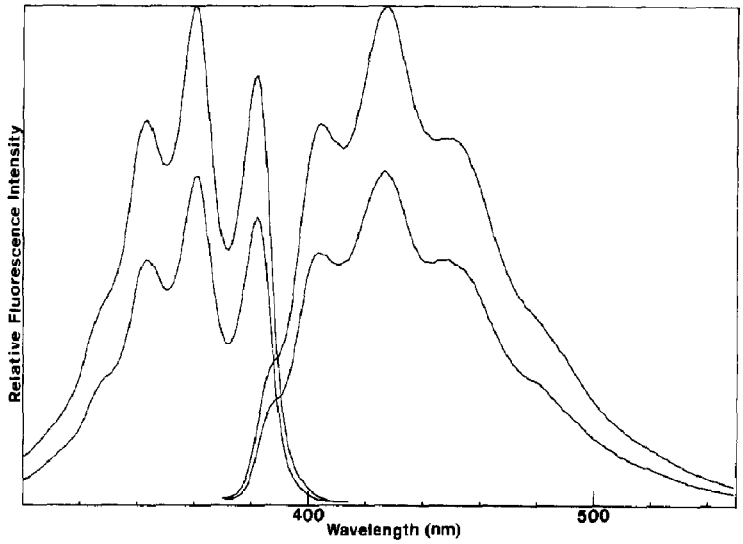

Fig. 3. Fluorescence excitation (left) and emission (right) spectrum of 10^{-6} M DPH embedded in 10^{-4} M DPPG small unilamellar vesicles in the absence (upper curves) and in the presence of 1.5×10^{-5} M 12-DSME (lower curves). The excitation wavelength for the emission spectrum was 350 nm with 2 nm emission slits. The emission wavelength for the excitation spectrum was 435 nm with 2 nm excitation slits.

Table 3

Data obtained by the analysis of the fluorescence decay profiles of 10^{-6} *M* DPH in the presence of 1.5×10^{-5} *M* 12-DSME in 10^{-4} *M* of DPPG–LαPG mixtures at 20°C, using eqs. (1)–(3)

Percentage LαPG	τ_0 (ns)	f	C_1/C_2	Rate constants (10^7 s^{-1})		
				K_1	K_{AV}	K_L
0	11.1	0.38	25	115	5.2	1.7
10	11.0	0.44	20	82	4.1	1.2
20	10.7	0.38	11	150	4.3	1.0
30	10.4	0.40	11	113	3.9	0.4
50	9.8	0.56	18	71	4.5	1.0
75	9.2	0.60	25	66	5.3	0.6
100	8.6	0.55	∞	81	8.2	4.4

does not depend on concentration. K_1 decreases with increasing temperature, same as it happens with pyrene, obviously, for the same reasons. On the contrary, K_L values cannot be considered zero anymore (of course, always, in comparison with the corresponding K_{AV} and K_1). This is a rather expected result since the time scale of the DPH measurements is much shorter than the one of pyrene. So what is long time for DPH, is still short time for pyrene. In other words, the diffusion distances monitored by DPH are much shorter. Note that K_L values increase with temperature. This means that the long-range diffusion (distance) is more probable at high temperature. For the same reason we also observed increase of the average rates K_{AV} with temperature.

Finally, Table 3 shows the results of the analysis of the fluorescence decay profiles of 10^{-6} *M* DPH in the presence of 1.5×10^{-5} *M* 12-DSME both solubilized in mixtures of DPPG and LαPG at 20°C. The phospholipid concentration was always 10^{-4} *M*. The percentage of the LαPG content is shown in the first column of Table 3. The long time component of the decay of DPH in pure LαPG is smaller than in pure DPPG. For this reason, τ_0 decreases in going from 0 to 100% LαPG. LαPG vesicles are in their LCP at 20°C. So it is not surprising that f increases with increasing LαAG content, even though, the results are now recorded with a rather large uncertainty. The surprising result is obtained with the values of C_1/C_2 which remain more or less invariable, to change abruptly in pure LαPG. Then only in pure LαPG is the number of available solubilization sites for the couple DPH–12-DSME large, while presence of even small percentages of DPPG excludes this facility. If we overlook the increased uncertainty of the information obtained by the data of Table 3, we note that, over all, the values of the K's behave the same way as with the two phases of DPPG obtained by varying temperature, i.e. K_1 decreases in going from GP to LCP, and K_L and K_{AV} increase.

4. Conclusion

When pure or mixed phospholipid vesicles undergo a transition from gel to liquid crystalline phase, either by changing temperature or by changing composition, then the reaction between a fluorophore and a quencher becomes less restricted and less local. For phospholipid concentration of 10^{-4} *M*, quasi-stationary reactions are expected only in the gel phase. The number of the available solubilization sites is larger in the liquid crystalline phase and it is particularly so for the couple DPH–12-DSME than it is for pyrene.

References

1 D. Daems, M. van der Zegel, N. Boens and F.C. de Schryver, Eur. Biophys. J. 12 (1985) 97.
2 G.P. L'Heureux and M. Fragata, J. Photochem. Photobiol. 3 (1989) 53.
3 B.M. Liu, H.C. Cheung, K.H. Chen and M.S. Habercom, Biophys. Chem. 12 (1980) 341.
4 J.M. Vanderkooi and J.B. Callis, Biochemistry 13 (1974) 4000.

5 G. Duportail, J.-C. Brochon and P. Lianos, J. Phys. Chem. 96 (1992) 1460.
6 P. Lianos, J. Chem. Phys. 89 (1988) 5237.
7 G. Duportail and P. Lianos, Chem. Phys. Lett. 149 (1988) 73.
8 G. Duportail and P. Lianos, Chem. Phys. Lett. 165 (1990) 35.
9 P. Lianos and P. Argyrakis, Phys. Rev. A 39 (1989) 4170.
10 P. Lianos and G. Duportail, Progr. Colloid. Polym. Sci. 84 (1991) 151.
11 P. Argyrakis, G. Duportail and P. Lianos, J. Chem. Phys. 95 (1991) 3808.
12 P. Lianos and G. Duportail, Eur. Biophys. J. 21 (1992) 29.
13 R. Rammal and G. Toulouse, J. Phys. Lett. 44 (1983) L13.
14 S. Havlin and D. Ben-Avraham, Adv. Phys. 36 (1987) 695.
15 R. Kopelman, J. Stat. Phys. 42 (1986) 185.
16 J. Klafter and A. Blumen, J. Chem. Phys. 80 (1984) 875.
17 Z. Huang and R.P. Haugland, Biochem. Biophys. React. Commun. 181 (1991) 166.
18 E. Blatt and W.H. Sawyer, Biochim. Biophys. Acta 822 (1985) 43.
19 T. Parassasi, F. Conti, M. Glaser and E. Gratton, J. Biol. Chem. 259 (1984) 14011.